MOA II Gravitational Microlensing Survey
— A new generation microlensing survey —

F. Abe[1], I. A. Bond[2], A. C. Gilmore[3], J. B. Hearnshaw[3] , Y. Itow[1], K. Kamiya[1]
P. M. Kilmartin,[3] , K. Masuda[1] , Y. Matsubara[1], Y. Muraki[4]
T. Sako[1], D. J. Sullivan[5]
P. Tristram[3], and P. C. M. Yock[6]

[1]*Solar-Terrestrial Environment Laboratory, Nagoya University, Nagoya*
Aichi 464-8601, Japan
[2]*Institute of Information and Mathematical Sciences, Massey University at Albany*
Auckland, New Zealand
[3]*Department of Physics and Astronomy, University of Canterbury*
Christchurch, New Zealand
[4]*Department of Physics, Konan University*
Kobe, Japan
[5]*School of Chemical and Physical Sciences, Victoria University*
Wellington, New Zealand
[6]*Department of Physics, University of Auckland*
Auckland, New Zealand

Abstract

Observing gravitational microlensing events has become a powerful technique for studying dark objects and the surface profiles of distant stars. The MOA II microlensing survey is a Japan-New Zealand collaboration that detects microlensing events towards the Galactic Bulge and the Magellanic Clouds. A recently installed 1.8-m wide-field telescope, equipped with a large CCD camera, enabled us to make high-cadence observations of most bulge microlensing events for the first time. This new type of microlensing survey opened new vistas in the search for planets by microlensing, and also in the search for MACHOs. In this paper we review past observations and science of microlensing, and then describe the MOA II project and its strategy.

1 Introduction

Gravitational microlensing is both a natural application of the general theory of relativity, and also a potentially powerful tool in astronomy. The concept of gravitational lensing [1] was introduced by Einstein in 1936. In his paper, Einstein predicted two phenomena. One was the "Einstein ring". If two stars are perfectly aligned on a line of sight, the rays of light from the more distant star are bent by the gravitational field of the nearer star. As the bending angle is independent of the azimuthal angle, the rays form a circular image, the so-called Einstein ring. If the stars are nearly aligned, a pair of arcs is produced. However, Einstein said in his paper, "Of course, there is no hope of observing this phenomenon directly." In spite of 70 year's progress in observational technology, Einstein rings (or arcs) are still difficult to observe. The resolution of the current largest optical interferometer VLTI (Very Large Telescope Interferometer) is 2.2 msec. This may be compared with the diameter of the Einstein ring which is typically less than 2 msec. To date, only one attempt has been made to directly resolve such an image [2, 3], and this was not successful [2]. The other phenomenon that Einstein predicted was magnification. This is the apparent increase in brightness of the distant star caused by the gravitational lensing of the nearer star, when the integrated light of the Einstein ring or arcs is detected. This phenomenon was also thought to be difficult to observe. Einstein said "Therefore, there is no great chance of observing this

[1]E-mail:abe@stelab.nagoya-u.ac.jp
[2]However, Einstein arcs and rings have been observed with aligned galaxies, for which the characteristic angle is of order secs [4]

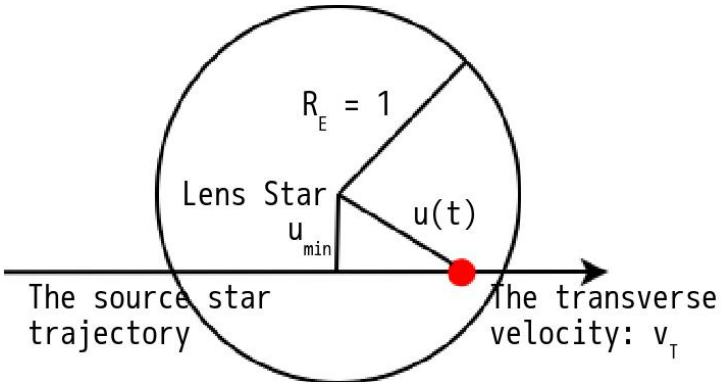

Figure 1: Configuration and definitions of parameters of a single lens event.

phenomenon, even if dazzling by the light of the much nearer star B is disregarded." However, modern technology now permits us to observe hundreds of microlensing events annually through the magnification effect.

The microlensing technique has been applied in a number of areas of astronomy. Because the effect is independent of the luminosity of the nearer star (i.e., the lens star), the technique can be applied to search for dark objects that are very difficult to detect by other means. Such dark objects might be, for example, MAssive Compact Halo Objects (MACHOs) [5], black holes [6], brown dwarfs, free-floating planets, and extrasolar planets. Microlensing can also be used to probe the more distant star (i.e., the source star). The magnification caused by microlensing depends sensitively on the angular separation between the lens and source stars, especially when the separation is small and the magnification is high. This enables the surface profile of a distant star to be resolved with remarkably high precision, allowing its atmosphere to be probed [7] or, in one case, its shape to be determined [8].

The search for MACHOs using microlensing [9] was originally proposed by Paczyński. If the stars in an external galaxy can be resolved, dark objects in the Halo in our galaxy may cause gravitational microlensing of them. This could be detectable through a change of the brightness of a resolved star. The magnification $A(t)$ by a single lensing object is

$$A(t) = \frac{u(t)^2 + 2}{u(t)(u(t)^2 + 4)^{1/2}}, \tag{1}$$

where, $u(t)$ is the projected distance between the source and the lens (see Fig.1),

$$u(t) = (u_{min}^2 + (v_T(t - t_0)/R_E)^2)^{1/2}, \tag{2}$$

u_{min} is the minimum $u(t)$, t_0 is the time of minimum, and R_E is the Einstein ring radius,

$$R_E^2 = \frac{4GMD}{c^2}, D = \frac{D_l D_{ls}}{D_s}, \tag{3}$$

where, G is the gravitational constant, M is the mass of the lens, c is the velocity of light, and D_l, D_{ls}, D_s are the distances between the observer and the lens, the lens and the source, the observer and the source, respectively. The variation of the brightness with time, i.e. the light curve, is symmetric before and after the peak (at t_0) and it is achromatic. The timescale of the event is characterized by the Einstein radius crossing time $t_E = R_E/v_T$. Typical values of t_E depend primarily on the masses of possible lenses, and are estimated to be $t_E > 200days$ for black holes, $6 < t_E < 150days$ for stars, $2 < t_E < 6days$ for brown dwarfs, and $t_E < 2days$ for planetary mass objects. As the time scales of most of events are expected to be several days or more, most past microlensing surveys included only one or a few observations/night.

The probability for a microlensing event to occur is expressed by the optical depth τ. Here τ is the probability for microlensing to occur on a star at a given instant. If the mass density of the lensing objects $\rho(D_l)$ is known, then τ can be deduced from the relationship

$$\tau = \int_0^{D_s} \frac{4\pi GD}{c^2} \rho(D_l) dD_l. \tag{4}$$

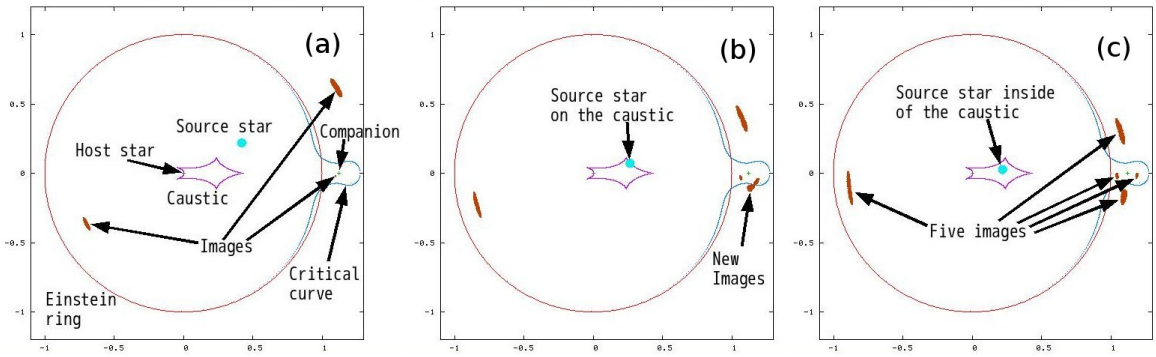

Figure 2: Configuration of binary lensing projected to the lens (host star and a companion) plane. When the source star is outside of the caustic (a), the number of images is 3. If the source star is on the caustic (b), new images appear. If the source star is inside of the caustic (c), the number of images is 5.

Typical estimated values of τ are $\sim 10^{-6}$. This implies that more than 10^6 stars must be monitored to find microlensing events. Thus, observations must be carried out toward crowded stellar fields (Magellanic Clouds, Galactic Bulge, or other galaxies), and wide-field surveys are necessary.

Using Paczyński's scheme, first generation surveys were performed to search for any dark matter in the form of MACHOs. These were conducted by MACHO (MAsive Compact Halo Object) [5], EROS (Expérience pour la Recherche d'Objects Sombres) [10], and OGLE (Optical Gravitational Lensing Experiment) [11]. Microlensing events towards the Large Magellanic Cloud (LMC) were reported by the MACHO and EROS groups, and toward the Galactic Bulge by the OGLE group. Since then, more than 3,000 microlensing events have been discovered, mostly in bulge fields. As the number density of stars in our Galaxy increases as the stellar mass decreases, the majority of microlensing events in the Galactic Bulge are expected to be caused by lenses that are low-mass red dwarfs.

A large fraction of the stars in our galaxy have companions. Such binary stars are expected to act as lenses for microlensing events too. But the magnification by a binary lens is complex compared with that of a single lens. The rays of light are bent by the host and the companion stars and are folded by each other. The magnification pattern on the source plane is divergent on closed lines named caustics. If the source star passes over a caustic, the light curve is singular. The magnification caused by binary lensing can be calculated by solving the lens equation,

$$\boldsymbol{\beta = \theta - \left(q_1 \frac{\theta}{|\theta|^2} - q_2 \frac{\theta - l}{|\theta - l|^2} \right)} \tag{5}$$

where, β is the source position vector projected onto the lens plane in units of R_E, θ is the image position vector, l is the position vector of the companion (the host star is assumed at the origin), and q_1 and q_2 are the mass ratio of the host star and the companion, respectively. Solutions [12] to Eq. 5 were obtained by Scheneider and Weiβ. Recently, a simpler method [13] was devised by Asada. Figure 2(a-c) show images for a binary configuration determined by Asada's method. As seen in the figures, there are three images when the source star lies outside the caustic. When the source star moves inside the caustic, the number of images becomes five. Integrating over the images, the magnification of the lens may be calculated. Alternatively, the Inverse-Ray Shooting (IRS) method may be used for binary and more complex lenses. In the IRS method, rays of light generated by a hypothetical point source at the position of the observer are traced through the lens to the source plane. The density of rays on the source plane represents the magnification.

The light curve for binary lensing is generally quite complex and asymmetric. If the lens star has a planet, the lens may be treated as a binary with a small mass ratio. The detectability of extrasolar planets by gravitational microlensing was first treated in this manner[14]. The method is particularly effective for finding planets in the "lensing zone" which is an annular region from 0.6 to 1.6 R_E centred on the lens star. In this region, the anomaly caused by a planet is amplified. Simulations show that planets down to Earth-mass or less [15, 16] could be discovered in this region. A typical Einstein ring radius is

$2-4AU$ in bulge microlensing events. This region corresponds to that occupied by the asteroid belt in our solar system. As mentioned above, most Galactic Bulge microlensing events are caused by low-mass red dwarfs, so planets orbiting such low-mass stars are the most common target of the microlensing method. Planets may thus be detected by microlensing in very different regions from those explored by the radial velocity and transit techniques.

In summary, the MOA II project aims to seek and identify a fraction of Galactic Dark Matter that may exist in the form of MACHOs, and also to seek and identify extrasolar planets by gravitational microlensing. The present paper is organized as follows. Our previous project, MOA I, is described in Sec. 2, and extrasolar planets in Sec. 3. The MOA II project is introduced in Sec. 4. This includes discussion of the observing strategy that is being used in MOA II. Finally, a summary is given in Sec. 5.

2 MOA I project

Japan-New Zealand collaboration MOA (Microlensing Observations in Astrophysics) project was started in 1995. The observations were done toward Magellanic Clouds because the primary target was the MACHO search. Due to the raising interest of extrasolar planet, observations toward Galactic bulge were started later. The observations were performed with use of 61 cm B & C telescope in Mt. John university observatory ($170.°28'E, 43.°59'S$), New Zealand. The first CCD camera was MOA-cam1 which had 9 $1k \times 1k$ TI chips. Large mosaic CCD camera MOA-cam2 [17] which had 3 $2k \times 4k$ SITe CCD chips was installed in 1998. One of the advantages of Mt. John is its unique location. Mt. John is the southernmost astronomical observatory in the world except for Antarctica. In winter (June and July), the Galactic bulge passes close to the zenith at midnight. Due to the high latitude, the bulge observation can be continued more than 13 hours. Mt. John is a good observation site for Magellanic Clouds too. Due to the high latitude, Magellanic Cloud don't set. Observations can be done anytime in clear nights.

In spite of the small aperture, MOA I obtained a number of scientific results: measurement of optical depth toward Galactic bulge [18], measurements of the atmosphere [19] and the shape [8] of a distant star, period-luminosity relation of long-period variables in LMC [20], Candidate of extrasolar planet transits [21], etc. The highlight of MOA I is discovery of the first extrasolar planet with microlensing [22]. We will mention this discovery in Sec. 3. The MOA I microlensing alert was started in 2000 and continued until 2005. The numbers of alerts were 13-74 alerts/year. After 10 years MOA I survey, MOA II took over microlensing survey.

3 Extrasolar planets

Finding planets outside of the solar system is one of the most exciting issues in current astronomy. Since first discovery [23] of extrasolar planet orbiting around a sun-like star, more than 200 planets [24] have been discovered. Most of them were discovered with radial-velocity method which detects periodic change of radial velocity of the host star caused by the planet. As this method is more sensitive to massive close-in planets, most of the planets discovered are massive or close-in planets. Discovery of a number of close-in giant planets named "hot Jupiters" raized discussions [25] wheter our solar system is special or not. However this question is hard to answere because access to low-mass wide orbit planets have been very difficult.

Looking back to our solar system, eight planets are orbiting around the sun. They can be categorized into three types: rocky (terrestrial) planets, gas giants (Jovian planets), and icy (uraniun) planets. Inner four planets (Mercury, Venus, Earth, and Mars) are rocky planets which have solid rocky surfaces. Jupiter and Saturn are gas giants which don't have solid surface and covered with hydrogen and helium gases. Outer two planets (Uranus and Neptune) are icy planets which have solid ice surfaces.

The standard model of the planet formation is the core-accretion model [26]. In this model, dusts in the protoplanetary disk are coagulated then formed kilo-meter size planetesimals. The main component of the dusts is expected to be silicates at inside and ice at outside (less than melding point). Thus the core of the planets are formed with rocks at inside and ices at out side. The planetesimals are collide each other and form larger objects named protoplanets. Planets are formed by giant collisions of protoplanets. At the final stage of planet formation, the cores of planets at right outside of the "snow line" absorb the

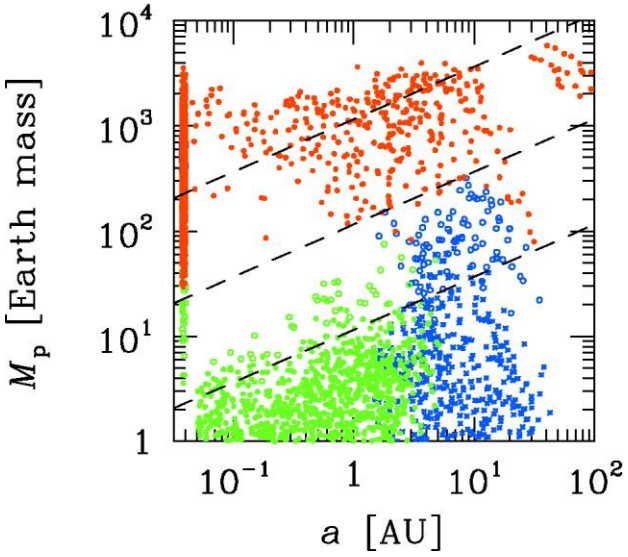

Figure 3: A result of a simulation [27] of the core-accretion model. Planet mass vs. semi-major axis. Red points represent gas giants, blue points are icy planets, and green points are rocky planets.

gas around them and gas giants are generated. This model succeeded to explain our solar system very well. A number of simulation studies have been made with this model. Figure 3 shows one of the results [27] of the simulation for a sun-like star. As shown in the figure, there are a number of rocky planets inside of the snow line ($\sim 2-3AU$) and icy planets in the outside. However, access to the low-mass rocky or icy planets was very difficult with conventional planet search. To confirm core-accretion model at extrasolar planetary system, new method has been necessary.

As we have mentioned, the microlensing planet search [14] was proposed by Mao and Paczyńscky in 1992. But the real discovery was difficult. After several pioneering attempt, the first extrasolar planet with microlensing [22] was discovered in 2003 by MOA I and OGLE. Anomaly in the light curve was discovered in OGLE 2003-BLG-235/MOA 2003-BLG-053 microlensing event. Figure 4 shows the light curve of OGLE 2003-BLG-235/MOA 2003-BLG-053. From the detailed analysis of the light curve, the mass ratio of the planet and the host star was determined to be $0.0039^{+0.0011}_{-0.0007}$ and separation to be 1.120 ± 0.007. To determine absolute values of the masses and the separation, determination of the distance to the lens system is necessary. As the determination of the distance from the observations is very difficult, the first estimate was done using stochastic method with a Galactic model. The obtained values were about $1.5M_J$ for the planet mass and about $3AU$ for the separation. In 2006, Hubble Space Telescope observed [28] the motion of the host star, then the proper motion and the distance were constrained. Using this constraint, the planet mass and the separation were better determined to be $2.6^{+0.8}_{-0.6}M_J$ and $4.3^{+2.5}_{-0.8}AU$, respectively. The microlensing planet search is thought to be potential method to discover down to earth-mass planet or less [15, 16]. But the first discovery was still a giant planet.

4 MOA II project

The MOA II project was started in 2002. New telescope which has 1.8-m aperture was installed in Mt. John Observatory in 2004. Figure 5 shows the 1.8-m telescope and the dome. To achieve very wide field of view, a prime focus optics with a parabolic primary mirror and four corrector lenses was adopted (see Fig. 6). This optics was effective to make wide-field telescope in a limited cost, because making primary mirror become much easier than short-focal length Ritchey-Crétien optics and no secondary mirror was needed. A new CCD camera named MOA-Cam3 [29] which has 10 $2k \times 4k$ E2V CCD chips was installed at the focal point. Figure 7 shows MOA-cam3 CCD camera. This system has strong advantages compared

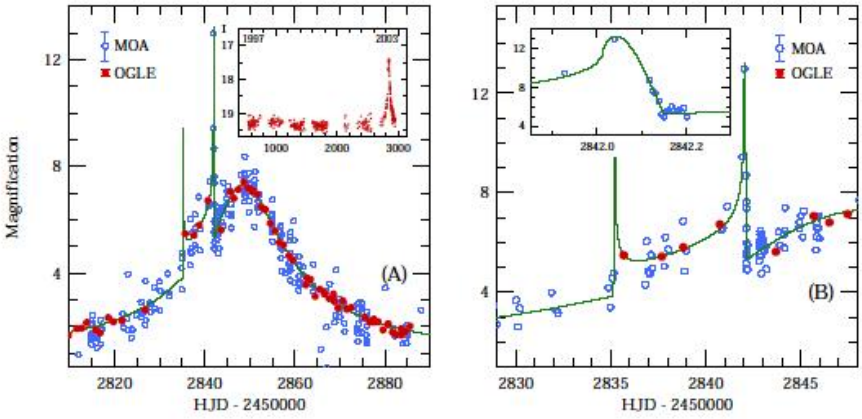

Figure 4: Discovery of first extrasolar planet with microlensing. The light curve of the microlensing event OGLE 2003-BLG-235/MOA 2003-BLG-053 [22] is shown. Two sharp peaks are caused by caustic crossing.

to past and on-going microlensing surveys. Table 1 shows comparison of the performances of microlensing surveys. The field of view was $2.2 degree^2$ which is about 6 times wider than that of OGLE. This wide field of view enabled us to take new observation strategy: high-cadence observation. There are two kinds of strategies in microlensing planet search: high magnification and high-cadence observations for all of the events. The difference of the strategies is due to the shape of the caustics of the planetary microlensing.

Figure 8 shows a magnification pattern of a planetary lensing. There are two kinds of caustics in the planetary lensing: central caustics and planetary caustics. The central caustics are always around the host star, thus the anomaly by the central caustics always appear [30] around the peak of high-magnification event. On the other hand, planetary caustics are hard to predict where they are. That means predicting anomaly is impossible for the planetary caustics. To detect anomaly caused by central caustics, watching peaks of high-magnification events is a clear very efficient strategy because observers can be concentrated into limited number of events and limited time. Once such event is discovered, no large CCD cameras are required. There are four major groups in microlensing observations: OGLE, MOA, PLANET/ROBOnet, and μFUN. In these groups, OGLE and MOA have large CCD cameras and working on microlensing event surveys. As the primary target is to find microlensing events, most of the telescope times are used for the microlensing survey. The other groups PLANET/ROBOnet and μFUN are working on follow-up observations of the events discovered by OGLE and MOA. These observations are done in target of opportunity base and no large CCD camera is used. Thus their observations are concentrated around the peaks of high-magnification events and specific target events they are interested in.

Table 1: Comparison of microlensing surveys

	MACHO	EROS	OGLE	MOA I	MOA II
Aperture (m)	1.27	1.0	1.3	0.61	1.8
FOV (deg^2)	0.5	0.938	0.325	1.27	2.18
Site	Australia	Chile	Chile	NZ	NZ
Status	Finished	Finished	Active	Finished	Active

In spite of the effectiveness of the high-magnification strategy, this method is thought to be inefficient to find low-mass planets. The size of the central caustic is proportional [31] to the mass ratio q and shrinks quickly with the mass ratio decrease. On the other hand, the size of the planetary caustics are

Figure 5: MOA II 1.8 m telescope at its opening ceremony.

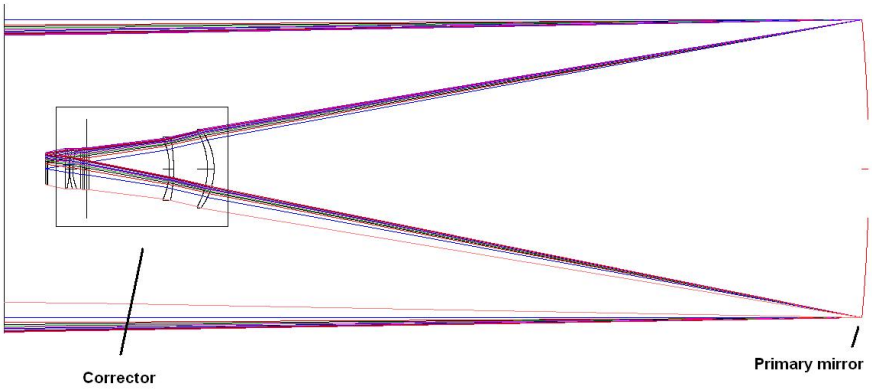

Figure 6: Optics of the MOA II telescope. A simple prime focus with a parabolic primary mirror and for corrector lenses was adopted.

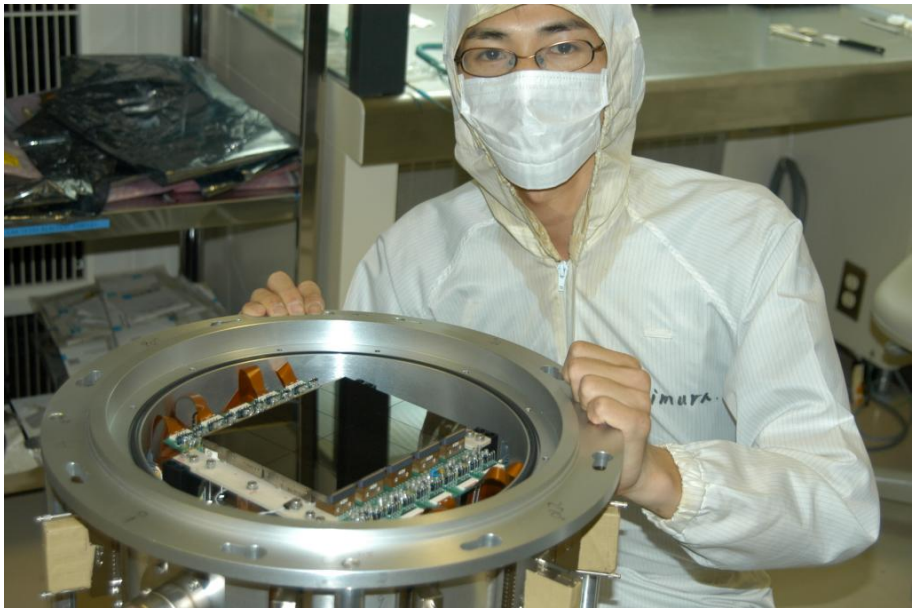

Figure 7: A large CCD camera MOA-cam3. The effective area is $12cm \times 15cm$.

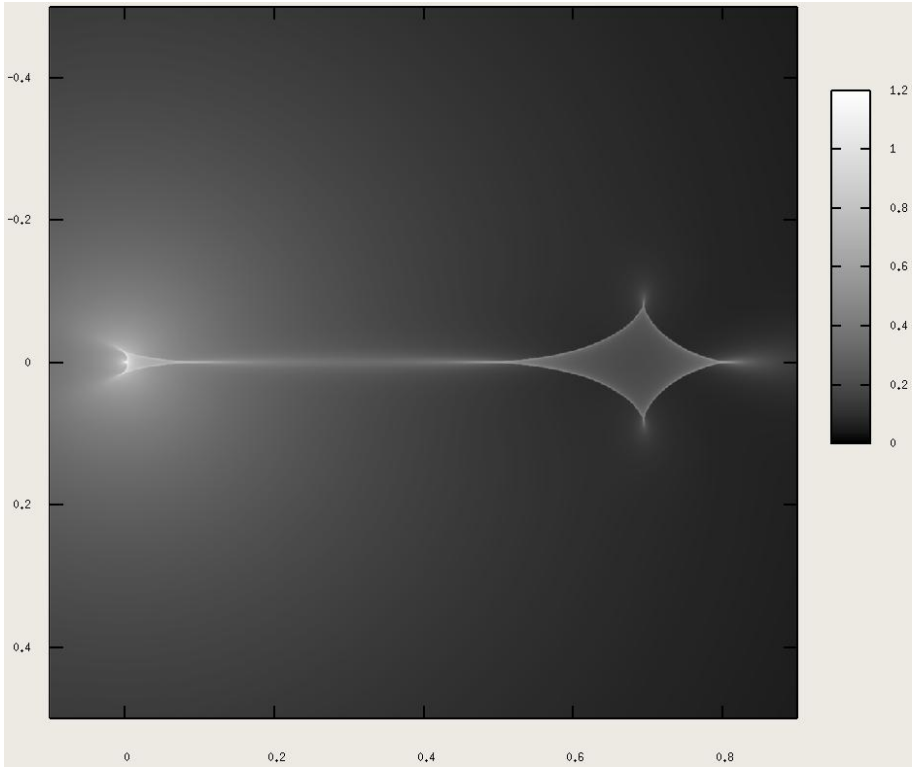

Figure 8: A magnification pattern of a planetary lensing. The host star is at origin, and the separation of the planet is 1.4 (outside of this figure). The mass ratio is 0.01. The small wedge shape caustic (left) is the central caustic and a large diamond shape caustic (right) is the planetary caustic.

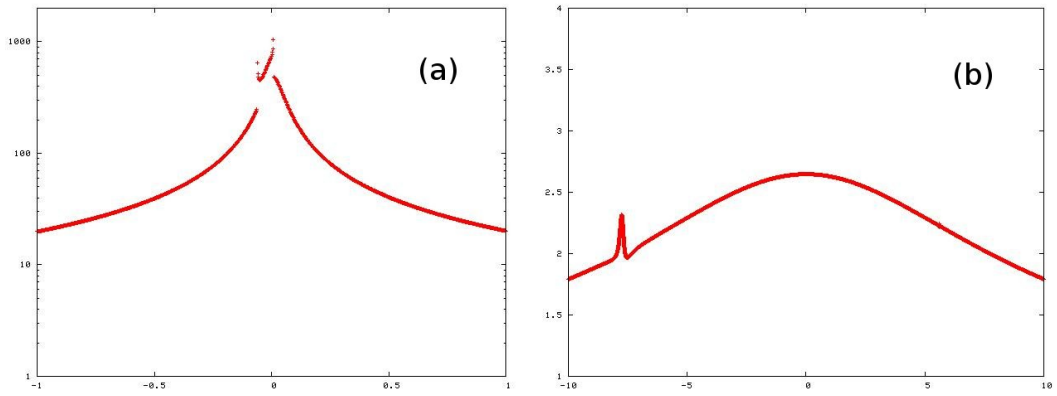

Figure 9: Light curves of a central caustic event (a) and a planetary caustic event (b). The anomaly by a central caustic always appear around the peak of a high-magnification event. The anomaly by a planetary caustic is hard to predict.

proportional [32] to the square root of the mass ratio. Anomaly shrinks both in time and change of brightness as the size of the caustic decrease. Thus finding planetary caustics are expected to be more efficient than finding central caustics. However, finding planetary caustic is more difficult because there is no prediction of anomaly to appear. Taking strong strategy such as high magnification is impossible to find planetary anomaly. Simply watching most of the events almost uniformly in time is only possible strategy. In this scheme, wider field of view is more efficient because higher-cadence observation can be done for most of the microlensing events.

The MOA II observation has started in 2005. The observations are being done for the 22 Galactic bulge fields. The exposure time is 60 seconds each. These 48 $degree^2$ are scanned every one hour. To find very short anomaly caused by low-mass planet, central 2 fields are observed every 10 minutes. A real time analysis is beeing done to find microlensing events on time. To find microlensing events efficiently, a Difference Image Analysis (DIA) [33] is used in the real time analysis. The MOA II microlensing alert system has started in 2006 for the Galactic bulge fields. The number of events were 168 in 2006 and 488 in 2007.

In 2005, an exciting microlensing event OGLE 2005-BLG-390 [34] was occurred. Figure 10 shows the light curve of this event. As seen in the figure, a small bump appeared on a single lens curve. From detailed analysis of the light curve, the bump is found to be caused by a low-mass planet. The mass of the planet was estimated to be $5.5^{+5.5}_{-2.7}M_{\oplus}$ and the separation to be $2.6^{+1.5}_{-0.6}AU$, where $M_{\oplus}$ is the mass of the Earth. At that time, it was the lowest mass planet discovered outside of the solar system. The host star was a low-mass ($M = 0.22^{+0.22}_{-0.11}M_{\odot}$) M dwarf. Combined with the separation, the surface temperature was estimated to be $\sim 50K$, a cool icy planet. It is the first discovery of extrasolar icy planet. MOA II succeeded to observe second peak caused by the planetary caustic. That means the MOA II wide-field survey itself can be a powerful follow-up observation for most of the microlensing events. The discovery of the low-mass planet shows possibilities of discovery of Earth-mass planet with microlensing in near future.

In spite of the microlensing surveys by MACHO and EROS groups, the fraction of MACHOs in the Galactic halo is still not well determined and a controversial issue in the dark matter problems. In 2000, the MACHO group reported [35] that the fraction of MACHOs is 20% for a typical halo model with a 95% confidence interval of 8%-50%. Although some of them were found to be variable stars, the reanalysis [36] of the data showed that the MACHO fraction is still 0.16 ± 0.06. On the other hand, EROS group reported a microlensing event in LMC previously. However they reported later that the events are not due to the microlensing but a variable star. They analyzed all of their LMC data and concluded that they have no candidate and set an upper limit [37] to the MACHO fraction. Figure 12 shows the final result of EROS group and that of MACHO group for comparison. As shown in the figure, there are discrepancies between EROS and MACHO results although a common small allowed region around $0.2 < M < 1.0$ and $0.05 < f < 0.1$. In addition, there are lots of discussions about the locations of the lensing objects:

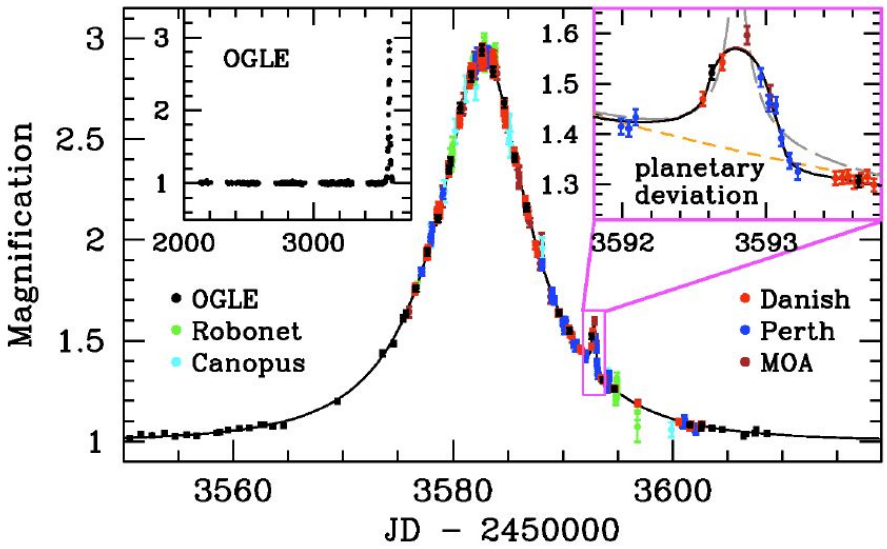

Figure 10: Discovery of first extrasolar icy planet. Light curve [34] of the microlensing event OGLE 2005-BLG-390 is shown.

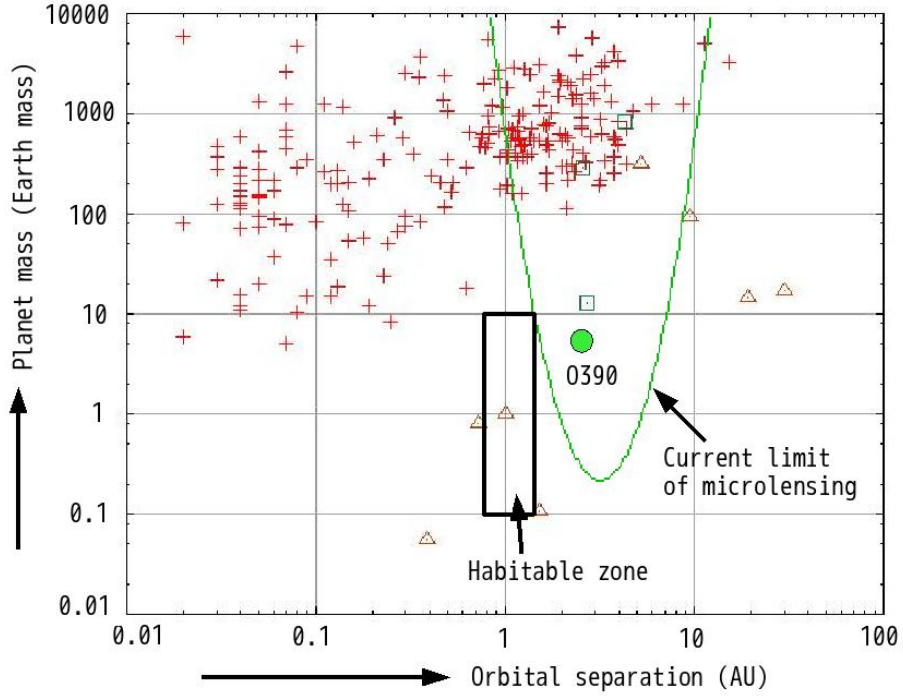

Figure 11: Extrasolar planets discovered with radial velocity and microlensing. The planet masses vs. the orbital separations are shown. The red crosses are discoveries with radial velocity method. Green squares are discoveries with microlensing. The brown triangles show solar system planets. The green circle is the planet discovered in OGLE 2005-BLG-390.

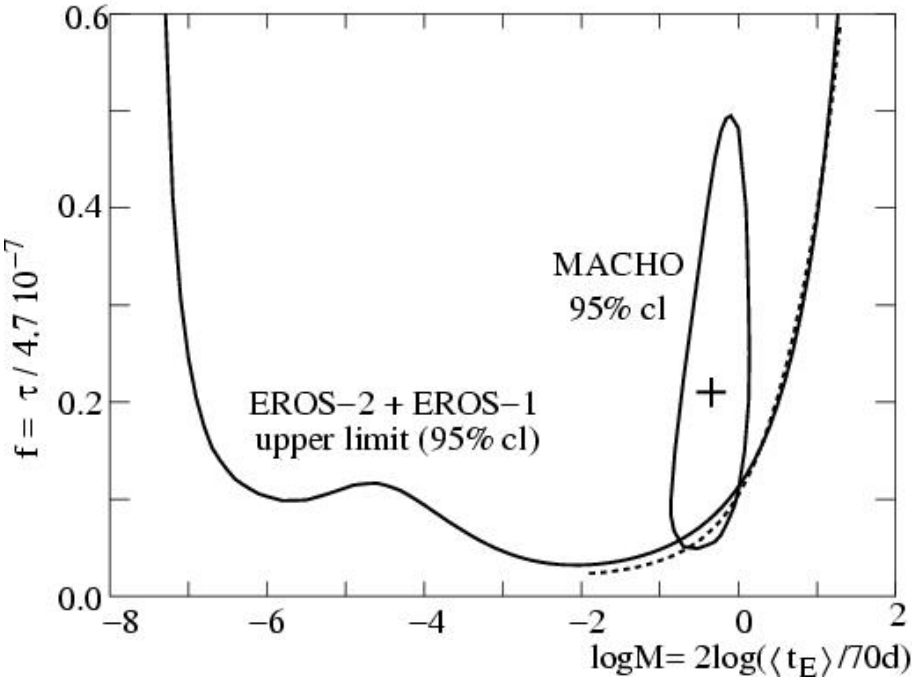

Figure 12: Results of past microlensing surveys toward Magellanic Clouds. The fraction [37] of MACHOs in the Galactic halo vs. the mass are shown. The 95% cl allowed area imposed by MACHO group and 95% cl upper limit imposed by EROS group are shown. The solid lines show LMC results. The dased line show EROS result including a SMC event.

lensings by MACHOs or lensing by LMC stars.

One of the aims of the MOA II project is to solve the MACHO problem and obtain well constrained value of the MACHO fraction. There are several advantages in MOA II to study MACHOs compared to other groups. The larger aperture enables us to observe more stars then to obtain more statistics of the microlensing events. The wide field of view enables us high-cadence observations to obtain well sampled light curves. Well sampled light curves are useful to discriminate background supernovae as well as variable stars. The locations of the lensing objects can be expected to be inferred from detailed analyses of the light curves if the parallax or finite source effect takes place. Well sampled light curves are useful for such analyses too. The high-sampled data around the peak of microlensing events are useful to find finite-source effects. From the analyses of finite-source effects, distances to the lens objects can be constrained. Durations of anomalies caused by finite-source effect are expected to be several hours to several days. In the past surveys, observations have been limited to a few times per night. Detecting short anomalies have been difficult. We are observing 14 LMC fields and 2 SMC fields in 300 second exposure time each. The central three fields are being observed every 30 minutes, while other fields are observed a few times every night. The MOA II survey is expected to obtain high sampled well constrained results in the MACHO problems.

5 Summary

Thanks to progress made in recent years in modern CCD technology, microlensing observations have become a powerful tool in astronomy. Observations of microlensing have been applied to seek dark objects and to probe distant stars. The first planet detection by microlensing was made jointly by MOA I and OGLE. Following this discovery, the method has matured and become a powerful method for planet hunting. Observations with the 1.8-m MOA II telescope commenced in 2005 using the MOA-cam3 CCD camera. Its wide field of view is being utilized to carry out high-cadence observations towards the Galactic Bulge and the Magellanic Clouds. This observational strategy has opened new channels for planet discovery, including the discovery of low-mass planets. The discovery of a 5.5 Earth-mass planet in OGLE 2005-BLG-390 event confirmed the efficacy of the high-cadence strategy. In the MACHO search, high-cadence observations toward the LMC and the SMC are expected to impose strict constraints on the fraction of MACHOs in halo of our galaxy.

The MOA II project is supported by the Ministry of Education, Culture, Sports, Science and Technology (MEXT), the Japan Society for Promotion of Science (JSPS), and the Marsden Fund of New Zealand.

References

[1] Einstein, A., Science 84, 506, 1936.

[2] Delplancke, F., Górski, K. M., Richichi, A., A & A 375, 2001.

[3] Rattenbury, N. J., Mao, S., MNRAS 365, 792, 2006.

[4] Cahntry, V. and Magain, P., A & A 470, 467, 2007.

[5] Alcock, C. et al., Nature 365, 621, 1993.

[6] Bennett, D. P., ApJ 579, 639, 2002.

[7] Alcock, C. et al., ApJ 491, 436, 1997.

[8] Rattenbury, N. J. et al., A & A 439, 645, 2005.

[9] PaczyńNatureski, B., ApJ 304, 1, 1986.

[10] Aubourg, E. et al., Nature 365, 623, 1993.

[11] Udalski, A. et al, Acta Astron. 43, 289, 1993.

[12] Scheneider, P. and Weiβ, A., A & A 164, 237, 1986.

[13] Asada, H., A & A 390, L11, 2002.

[14] Mao, S. and Paczyński, B., ApJ 374, 37, 1991.

[15] Bennett, D. P. and Rhie S. H., ApJ 472, 660, 1996.

[16] Dominik, M. et al., MNRAS 380, 792, 2007.

[17] Yanagisawa, T. et al., Exper. Astron. 10, 519, 2000.

[18] Sumi, T. et al., ApJ 541, 204, 2003.

[19] Abe, F., A & A 411, L493, 2003.

[20] Noda, S. et al., MNRAS 330, 137, 2002.

[21] Abe, F. et al., MNRAS 364, 325, 2005.

[22] Bond I. A. et al., ApJ 606, L155, 2004.

[23] Major, M. and Queloz, D., Nature 378, 355, 1995.

[24] Schneider, J., http://exoplanet.eu/

[25] Beer, M. E. et al., MNRAS 354, 763, 2004.

[26] Kokubo, E., and Ida, S., ApJ 581, 666, 2002.

[27] Ida, S. and Lin, D. N. C., ApJ 616, 567, 2004.

[28] Bennett, D. P., et al., ApJ 647, L171, 2006.

[29] Sako, T. et al., Exper. Astron., to be published.

[30] Griest, K., and Safizadeh, N., ApJ 500, 37, 1998.

[31] Chung, S.-J. et al., ApJ 630, 535, 2005.

[32] Han, C., ApJ 638, 1080, 2006.

[33] Bond, I. A. et al., MNRAS 327, 868, 2001.

[34] Beaulieu, J.-P. et al., Nature 439, 437, 2006.

[35] Alcock, C. et al., ApJ 542, 281, 2000.

[36] Bennett, D. P., ApJ 633, 906, 2005.

[37] Tisserand, P. et al., A & A 469, 387, 2007.